X-ray Absorption and X-ray Magnetic Dichroism Study on Ca_3CoRhO_6 and Ca_3FeRhO_6

Using X-ray absorption spectroscopy at the Rh-, Co-, and Fe-$L_{2,3}$ edges, we find a valence state of Co^{2+}/Rh^{4+} in Ca_3CoRhO_6 and of Fe^{3+}/Rh^{3+} in Ca_3FeRhO_6. X-ray magnetic circular dichroism spectroscopy at the Co-$L_{2,3}$ edge of Ca_3CoRhO_6 reveals a giant orbital moment of about 1.7 μ_B, which can be attributed to the occupation of the minority-spin d_0d_2 orbital state of the high-spin Co^{2+} ($3d^7$) ions in trigonal prismatic coordination. This active role of the spin-orbit coupling explains the strong magnetocrystalline anisotropy and Ising-like magnetism of Ca_3CoRhO_6.

The quasi one-dimensional transition-metal (TM) oxides Ca_3ABO_6 (A = Fe, Co, Ni, …; B = Co, Rh, Ir, …) have attracted a lot of interest in recent years because of their unique electronic and magnetic properties. The structure of Ca_3ABO_6 contains one-dimensional (1D) chains consisting of alternating face-sharing AO_6 trigonal prisms and BO_6 octahedra. Each chain is surrounded by six parallel neighboring chains forming a triangular lattice in the basal plane. Peculiar magnetic and electronic behaviors are expected to be related to geometric frustration in such a triangle lattice with antiferromagnetic (AFM) interchain interaction and Ising-like ferromagnetic (FM) intrachain coupling.

Ca_3Co2O_6 shows stair-step jumps in the magnetization at regular intervals of the applied magnetic field of $M_s/3$ suggesting ferrimagnetic spin alignment. The measured magnetic susceptibility undergoes two transitions at T_{c1} = 24 K and T_{c2} = 12 K which were attributed to FM-intrachain and AFM-interchain coupling, respectively. Ca_3CoRhO_6 and Ca_3FeRhO_6 have the same crystal structure as Ca_3Co2O_6, but different magnetic and electronic properties. Ca_3CoRhO_6 has only one plateau at 4 T and two transition at T_{c1} = 90 K and T_{c2} = 25 K. In contrast, Ca_3FeRhO_6 has an AFM ordering below T_N = 12 K. In order to understand the magnetic properties of Ca_3FeRhO_6 and Ca_3FeRhO_6, and particularly origin of the intrachain magnetic coupling of quasi 1D systems, the valence, spin, and orbital states have to be clarified. However, these issues have been contradictorily discussed in previous theoretical and experimental studies. The GGA density-functional band calculations suggest a Co^{3+}/Rh^{3+} state in Ca_3CoRhO_6 while LSDA+U calculations favor a Co^{2+}/Rh^{4+} state and a giant orbital moment due to the occupation of minority-spin d0 and d_2 orbitals. Neutron diffraction experiments on Ca_3CoRhO_6 suggest the Co^{3+}/Rh^{3+}. However, the magnetic susceptibility and X-ray photoemission spectroscopy indicated Co^{2+}/Rh^{4+}. For Ca_3FeRhO_6, the Fe^{2+}/Rh^{4+} state

Beamlines

17A1 X-ray Powder Diffraction

15B1 BM-Tender

Authors

T. Burnus, Z. Hu, and L. H. Tjeng.

II. Physikalisches Institut, Universität zu Köln, Germany.

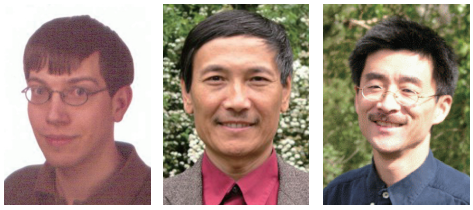

was suggested in a magnetic susceptibility study, whereas Mössbauer spectroscopy indicated a Fe^{3+} state, and thus Rh^{3+}.

Figure 1 shows the XAS spectra at the Rh-$L_{2,3}$ edges of Ca_3FeRhO_6 (dashed line) and Ca_3CoRhO_6 (solid line). The Rh-$L_{2,3}$ spectrum shows a simple, single-peaked structure at both Rh-L_2 and Rh-L_3 edges for Ca_3FeRhO_6, while an additional low-energy shoulder is observed for Ca_3CoRhO_6. Furthermore, the peak in the Ca_3CoRhO_6 spectrum is shifted by 0.8 eV to higher energies compared to that of the Ca_3FeRhO_6. The single-peaked spectral structure for Ca_3FeRhO_6 indicates Rh^{3+} ($4d^6$) with completely filled t_{2g} orbitals, i.e. only transitions from the 2p core levels to the e_g states are possible. The shift to higher energies from Ca_3FeRhO_6 to Ca_3CoRhO_6 reflects the increase in the Rh valence from Rh^{3+} to Rh^{4+} as we can learn from previous studies on 4d transition-metal compounds[1–3]. Furthermore, for Ca_3FeRhO_6 the spectrum shows a weak low-energy shoulder, which is weaker at the Rh-L_2 edge than at the Rh-L_3 edge. This shoulder can be attributed to transitions from the 2p core levels to the t_{2g} state, reflecting a $4d^5$ configuration with one hole at the t_{2g} state. Such spectral features were found earlier for Ru^{3+} in $Ru(NH_4)_3Cl_6$ [1]. Detailed calculations reveal that the multiplet and spin-orbit interactions suppress the t_{2g}-related peak at the L_2 edge for a $4d^5$ configuration[1–3]. Now we turn to the Fe-$L_{2,3}$ and the Co-$L_{2,3}$ XAS spectra to further confirm the Fe^{3+} state and the Co^{2+} state, as expected for charge balance.

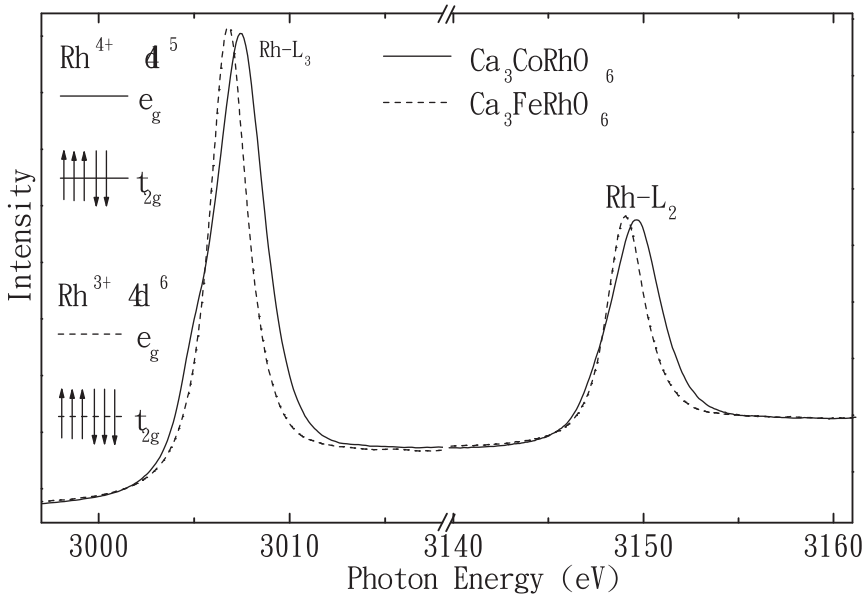

Fig. 1: The Rh-$L_{2,3}$ XAS spectra of Ca_3CoRhO_6 and Ca_3FeRhO_6 and a schematic energy level diagram for Rh^{3+} $4d^6$ and Rh^{4+} $4d^5$ configurations in octahedral symmetry.

Figure 2 shows the experimental Fe-$L_{2,3}$ XAS spectra of (g) Ca_3FeRhO_6 along with those of (a) single crystalline Fe_2O_3 as a Fe^{3+} reference and of (j) FeO as a Fe^{2+} reference. The calculated spectra for different symmetries using purely ionic (i.e. without Fe 3d–O2p hybridization) crystal-field multiplet calculations are shown. The main peak of the Fe-L_3 structure of the Ca_3FeRhO_6 lies 0.8 eV above the main peak of the divalent reference FeO and only slightly lower in energy than the one of Fe_2O_3. This indicates trivalent iron ions in Ca_3FeRhO_6.

The experimental spectra of the reference compounds, curve (a) for Fe_2O_3 and curve (j) for FeO can be well understood using the multiplet calculations in O_h symmetry, which are depicted in curve in Fig. 2(b) and Fig. 2(i) with t_{2g}–e_g splitting of 1.6 eV and 0.9 eV, respectively. In order to understand the experimental Fe-$L_{2,3}$ spectrum of Ca_3FeRhO_6, we first return to the Fe_2O_3 spectrum. When we reduce the t_{2g}–e_g splitting splitting from 1.6 eV (curve b) via 1.0 eV (curve c) to 0.0 eV (curve d), we observe that the low-energy shoulder becomes washed out, while the high-energy shoulder becomes more pronounced. Going further to a trigonal crystal field, the high-energy shoulder

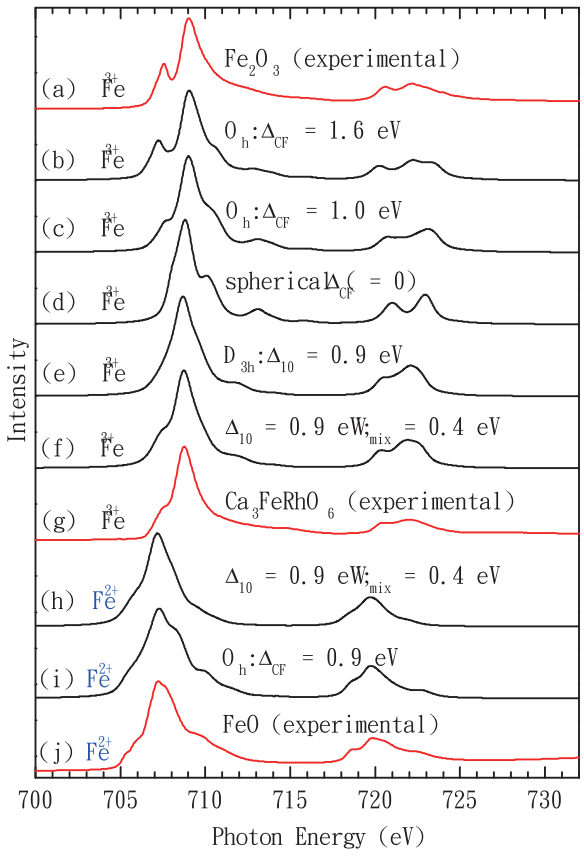

Fig. 2: Experimental Fe-$L_{2,3}$ XAS spectra of (a) Fe_2O_3 (Fe^{3+}), (g) Ca_3FeRhO_6, and (j) FeO (Fe^{2+}) together with simulated spectra (b, c) in O_h, (d) spherical, and (e, f) D_{3h} symmetry for Fe^{3+} and simulated spectra in (h) D_{3h} and (i) O_h symmetry for Fe^{2+}.

looses its intensity as shown in curve (e) for a splitting of 0.9 eV between $d_{\pm1}$ and $d_0/d_{\pm2}$. The experimental Fe-$L_{2,3}$ XAS spectrum of Ca_3FeRhO_6 can be well reproduced with this trigonal crystal field of 0.9 eV curve (f). and in addition a mixing parameter V_{mix} = 0.4eV, which mixes the $d_{\pm2}$ with the $d_{\pm1}$ orbitals.

To confirm this Co^{2+}/Rh^{4+} scenario for Ca_3CoRhO_6 we have to study explicitly the valence of the Co ion. Figures 3 shows the Co-$L_{2,3}$ XAS spectra of Ca_3CoRhO_6 together with CoO as a Co^{2+} and $Ca_3Co_2O_6$ as a Co^{3+} reference[4,5]. Again we see a shift to higher energies from CoO to $Ca_3Co_2O_6$ by about 1 eV. The Ca_3CoRhO_6 spectrum lies at the same energy position as the CoO spectrum confirming the Co^{2+}/Rh^{4+} state[6].

The magnetic properties of Ca_3FeRhO_6 are relatively simple as both the HS Fe^{3+} and LS Rh^{3+} ions have a closed subshell and thus no orbital degrees of freedom and no orbital moment. However, the orbital occupation and magnetic properties of Co^{2+} ($3d^7$) ion at the trigonal prism

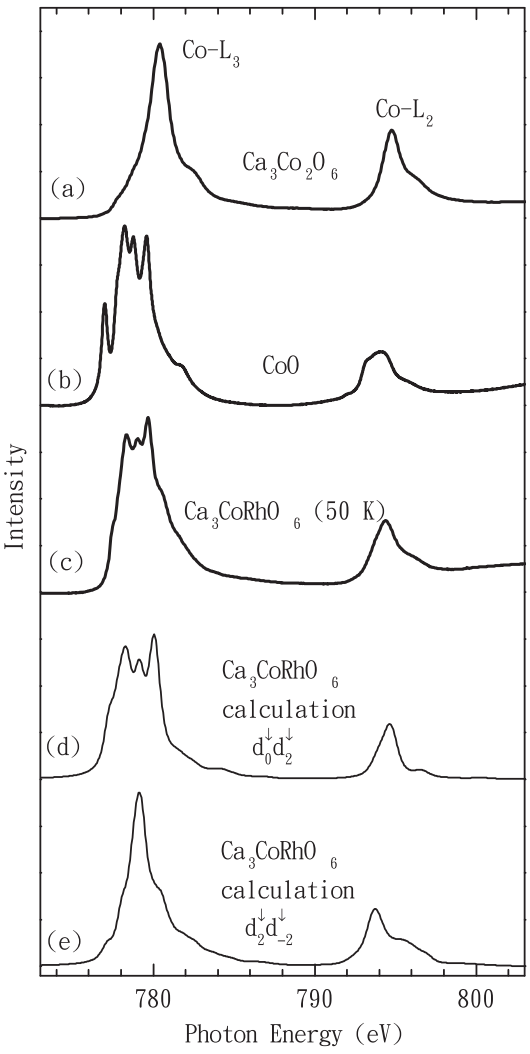

Fig. 3: The Co-$L_{2,3}$ spectra of Ca_3Co2O_6 (Co^{3+}) (a), CoO (Co^{2+}) (b), and Ca_3CoRhO_6(c). The simulated spectra of high-spin Co^{2+}($3d^7$) in trigonal prismatic symmetry for a d_0d_2 (d) and for a d_2d_{-2} (e) minority-spin orbital occupation.

site are more complicated.

In trigonal-prism symmetry the 3d orbitals are split into $d_{\pm1}$, d0, and $d_{\pm2}$ states. In terms of one-electron levels, the $d_{\pm1}$ orbitals lie highest in energy, while the lower lying d_0, and $d_{\pm2}$ states usually are nearly degenerate. For $Ca_3Co_2O_6$ with a Co^{3+} d^6 configuration, our previous experimental and theoretical works indicated that the $d_{\pm2}$ orbitals lie lower than d_0 orbital and one minority-spin occupation of d_2 orbital giving a giant orbital moment of 1,57 μ_B [4,5]. For Co^{2+} d^7 configuration, however, the situation is quite different. The double occupation of the d_0d_2 orbitals is energetically more favored than that of the d_2d_{-2}: the energy difference could be of order 1 eV [1], while the d_0 and $d_{\pm2}$ by themselves could be degenerate on a one-electron level. The consequences are straightforward: the double occupation of d_0d_2 should lead to a large orbital moment of 2 μ_B (neglecting covalent effects) and Ising type of magnetism with the magnetization direction fixed along the chains. In contrast, the double occupation of d_2d_{-2} would have given a quenched orbital moment. In Fig. 3(d) one clearly observes that the theory reproduces the experimental spectra very well with d_0d_2 orbital occupation, while it is very different from the experiment with d_2d_{-2} scenario (e) [7].◆

Experimental Station

XAS end station & X-ray absorption diffraction end station

References

1. F. M. F. de Groot, Z. Hu, M. F. Lopez, G. Kaindl, F. Guillot and M. Tronic, J. Chem. Phys. **101**, 6570 (1994).
2. Z. Hu *et al*., Phys. Rev. B **61**, 5262 (2000).
3. Z. Hu *et al*. Chem. Phys. **282**, 451 (2002).
4. T. Burnus *et al*., Phys. Rev. B **74**, 245111 (2006).
5. H. Wu, M. W. Haverkort, Z. Hu, D. I. Khomskii, and L. H. Tjeng, Phys. Rev. Lett. **95**, 186401 (2005).
6. H. Wu, Z. Hu, D. I. Khomskii, and L. H. Tjeng, Phys. Rev. B **75**, 245118 (2007).
7. T. Burnus *et al*., Phys. Rev. B **77**, 20511 (2008).

Contact E-mail

zhiwei@ph2.uni-koeln.de